

Interaction of the EWS NH₂ Terminus with BARD1 Links the Ewing's Sarcoma Gene to a Common Tumor Suppressor Pathway¹

Laura Spahn, Robert Petermann, Christine Siligan, Johannes A. Schmid, Dave N. T. Aryee, and Heinrich Kovar²

Children's Cancer Research Institute, St. Anna Kinderspital, 1090 Vienna, Austria [L. S., R. P., C. S., D. N. T. A., H. K.], and Department of Vascular Biology and Thrombosis Research, University of Vienna, 1235 Vienna, Austria [J. A. S.]

Abstract

In 85% of Ewing family tumors, the NH₂ terminus of EWS is fused to the DNA-binding domain of FLI1, an ets transcription factor. The resulting chimeric protein is a strong transcriptional activator with transforming activity. We report that EWS and EWS-FLI1 interact via their common NH₂ terminus with the COOH terminus of BARD1, a putative tumor suppressor, *in vitro* and *in vivo*. Because BARD1 associates via its NH₂-terminal RING domain with the breast cancer susceptibility gene *BRCA1* that provides a platform for interactions with proteins involved in DNA repair and checkpoint control, our results provide a link between the Ewing's sarcoma gene product and the genome surveillance complex.

Introduction

The TET family of genes encoding RNA-binding proteins EWS, TLS, and TAF_{II}68 is frequently involved in chromosomal translocations in human cancer (for review, see Ref. 1). TET proteins share common structural motifs, including copies of the degenerate hexapeptide motif SYGQQS in varying numbers, and a unique RNA-binding domain comprised of a RNP motif and RGG boxes. In EFTs,³ the *EWS* gene is fused to the ets transcription factor gene *FLI1* in 85% of cases. In the resulting chimeric protein, the putative RNA-binding portion of EWS is replaced by the DNA-binding domain of the ets transcription factor. In reporter gene assays, the NH₂-terminal EWS portion contributes significant transactivating activity when fused to a DNA-binding domain. However, in EWS-FLI1-transfected NIH3T3 cells, an approximately similar number of genes has been found to be repressed and activated by the fusion protein (2). EWS-FLI1 has transforming capacity *in vitro* and *in vivo*, requiring the EWS NH₂ terminus and the ets DNA-binding domain of FLI1. Most of the transforming potential resides in the first 82 amino acids of the EWS domain, distinct from the domain contributing the strongest transactivation potential (3). Because EWS-FLI1 derivatives lacking the DNA-binding domain still remain tumorigenic (4), it may be postulated that EWS-FLI1 plays a role in processes distinct from its DNA binding activity, presumably involving protein-protein interactions. The NH₂-terminal domain of EWS provides the interaction surface for association of EWS and EWS-FLI1 with components of RNA polymerase II and with splicing factors U1C and SF1, indicating a role for both proteins in transcription and RNA processing (for review, see Ref. 1). In fact, EWS-FLI1 has been demonstrated to alter hnRNPA1-dependent splice site selection *in vitro* (5).

In a yeast two-hybrid screen using the minimal EWS-transforming domain as a bait, we previously reported on the specific interaction of hsRBP7, a subunit of RNA polymerase II restricted to EWS-FLI1 but not to EWS (6). These data are compatible with an altered conformation of the EWS NH₂ terminus in the context of its fusion to FLI1 affecting protein-protein interaction characteristics that may contribute to its transforming function (7). We now report on a further interaction partner isolated from this screen, the BRCA1 associated RING domain protein BARD1. BARD1 not only interacts with BRCA1 but is also structurally related to this established tumor suppressor, implicating that it may act as a tumor suppressor as well (8). We show that, in contrast to hsRBP7, BARD1 interacts with both EWS and EWS-FLI1 *in vitro* and *in vivo*. Because BARD1 communicates with components of the BRCA1-associated genome surveillance complex, our findings may couple EWS and EWS-FLI1 to DNA repair and possibly also to checkpoint control.

Materials and Methods

Tissue Culture and Transfection. Cell lines used in this study were the EWS-negative EFT cell line STA-ET-7.2 (9), the neuroblastoma cell line SJ-NB7 (kindly provided by T. Look; St. Jude Children's Research Hospital, Memphis, TN), and HeLa (CCL2; American Type Culture Collection). Transfections were done with LipofectAMINE Plus reagent (Invitrogen, Groningen, the Netherlands), according to the manufacturer's instructions.

Plasmids. To generate GST fusion constructs, coding sequences of EWS-FLI1 type 1 and EWS were amplified by PCR and cloned into the pGEX-5X-1 vector (Amersham Biosciences, Uppsala, Sweden). For cytomegalovirus promoter-driven ectopic expression in mammalian cells, full-length cDNAs were cloned into pCMVneo (6) in the absence or presence of an NH₂-terminal double FLAG tag and a COOH-terminal c-myc tag. The constructs for FRET microscopy were generated by inserting the coding regions of BARD1, EWS, and EWS-FLI1 in-frame into the pECFP-C1 and pEYFP-C1 vectors (Clontech, Palo Alto, CA). The plasmid encoding the CYFP tandem fusion has been described previously (10).

GST Pull-down. GST fusion proteins were expressed in *Escherichia coli* XL1blueMRF⁻ after induction by isopropyl-1-thio-β-D-galactopyranoside for 2–5 h. The soluble protein fraction was coupled to glutathione-Sepharose 4B (Amersham Biosciences). *In vitro*-transcribed and -translated BARD1 and firefly luciferase proteins were synthesized in the presence of 20 μCi of [³⁵S]methionine/cysteine using the Proteinscript II kit (Ambion, Austin, TX) or the TNT T7 system (Promega, Madison, WI). Labeled proteins were incubated with 2 μg of GST proteins coupled to glutathione-Sepharose beads in 300 μl of Kleiman buffer (11) for 2 h at 4°C. Bound proteins were washed three times and analyzed on a 6% SDS-polyacrylamide gel, followed by autoradiography.

IPs. For IP of FLAG-tagged proteins, cells were harvested 48 h after transfection, and whole cell lysates were prepared in 400 μl of Kleiman buffer by two freeze/thaw cycles. Protein complexes were precipitated by incubation for 2 h at 4°C with Dynabeads M-450 (Dyna, Oslo, Norway) precoupled to anti-FLAG M2 antibody (Sigma, St. Louis, MO) or, for control, anti-CD99 hybridoma supernatant 12E7. For IP of endogenous protein complexes, cellular extracts were prepared either in modified radioimmunoprecipitation assay buffer containing 400 mM HEPES (pH 7.9; HeLa cells) or as described by Lassar *et al.* (Ref. 12; STA-ET-7.2 cells). Precipitations were carried out overnight at 4°C with protein G-Sepharose 4 Fast Flow (Amersham Bio-

Received 5/14/02; accepted 6/28/02.

The costs of publication of this article were defrayed in part by the payment of page charges. This article must therefore be hereby marked *advertisement* in accordance with 18 U.S.C. Section 1734 solely to indicate this fact.

¹ Supported in part by Grants 13708-GEN and 14299-GEN of the Austrian Science Foundation (to H. K.).

² To whom requests for reprints should be addressed, at Children's Cancer Research Institute, St. Anna Kinderspital, Kinderspitalgasse 6, A-1090 Vienna, Austria. Phone: 43-1-40470, ext. 409; Fax: 43-1-4087230; E-mail: kovar@ccri.univie.ac.at.

³ The abbreviations used are: EFT, Ewing's sarcoma family tumor; GST, glutathione S-transferase; FRET, fluorescence resonance energy transfer; CFP, cyan fluorescent protein; YFP, yellow fluorescent protein; IP, immunoprecipitation.

sciences) using the antibodies anti-KAI (Santa Cruz Biotechnology, Santa Cruz, CA) and anti-BARD1 669D and EE6 (kindly provided by R. Baer). After extensive washing, precipitated proteins were resolved on 8.5% SDS-polyacrylamide gels followed by Western blotting. Proteins were detected by the following antibodies: monoclonal anti-FLAG M2 (Sigma); rabbit anti-BARD1 polyclonal sera 669D or 58E (provided by R. Baer); rabbit anti-EWS serum 138-2 (provided by C. T. Denny); mouse hybridoma anti-FLI1 supernatant 7.3 (provided by O. Delattre); rabbit anti-FLI1 polyclonal antibody C19 (Santa Cruz Biotechnology); or anti-BRCA1 polyclonal antibody C20 (Santa Cruz Biotechnology). Primary antibodies were detected by horseradish peroxidase-conjugated secondary antibodies and SuperSignal WestPico chemiluminescent substrate (Pierce, Rockford, IL).

FRET Microscopy. SJ-NB7 cells were seeded on round coverslips and transfected with the indicated expression plasmids. Forty-eight h after transfection, cells were fixed with 2% formaldehyde. For FRET microscopy, the coverslips were placed in a chamber, covered with PBS, and analyzed with a Nikon Diaphot TMD microscope equipped with filter sets that discriminate between CFP and YFP fluorescence (Omega Optical Inc., Brattleboro, VT; CFP filter set: excitation 440 nm, dichroic mirror 455 nm, emission 480 nm; YFP filter set: excitation 500 nm, dichroic mirror 525 nm, emission 535 nm). Images were taken with a cooled charge-coupled device camera (Kappa GmbH, Gleichen, Germany). Acceptor photo-bleaching FRET microscopy was done by continuous illumination with a 100 W mercury lamp for 50 s and the YFP filter set. A CFP filter image was taken before and after photo-bleaching under identical conditions. The increase in donor fluorescence after acceptor photo-bleaching was calculated by dividing the CFP image after photo-bleaching (CFPpost) by the CFP image before photo-bleaching (CFPpre) using NIH Image software version 1.62.

Results

BARD1 Interacts with the EWS NH₂ Terminus in Yeast. A yeast two-hybrid screen was performed to identify proteins that interact specifically with the 82 NH₂-terminal amino acids of EWS, as reported previously (6). One of the clones isolated in this screen encoded for amino acids 427–777 of the BRCA1-associated RING domain protein BARD1. This domain contains two of the three ankyrin repeats and the BRCT tandem domain in the COOH terminus but lacks the NH₂-terminal RING finger domain of BARD1. The BARD1 portion did not activate the reporter genes *lacZ* or *HIS3* in absence of the Δ EWS-bait, excluding the possibility of a false-positive or nonspecific interaction.

BARD1 Interacts with EWS and EWS-FLI1 *in Vitro*. To confirm the interaction between the BARD1 COOH terminus in the context of full-length EWS and EWS-FLI1, *in vitro* pull-down assays were performed using bacterially expressed GST fusion proteins for EWS and EWS-FLI1 with *in vitro*-translated and radiolabeled full-length BARD1 or, for negative control, firefly luciferase. Both proteins, GST-EWS and GST-EWS-FLI1, retained BARD1, confirming the ability of full-length BARD1 to associate with proteins containing the EWS NH₂ terminus. Because BARD1 did not bind to GST-only and, in addition, the nonrelated control protein firefly luciferase did not bind to the GST fusion proteins, the interaction was considered to be specific (Fig. 1).

BARD1 Interacts with EWS and EWS-FLI1 in Cellular Extracts. To demonstrate the association of BARD1 with EWS and EWS-FLI1 expressed in human cells, we precipitated the two complexes from transiently transfected SJ-NB7 cells. Because of highly unselective binding of EWS and EWS-FLI1 to protein G-Sepharose, we chose magnetic Dynabeads coated with the secondary antibody as precipitation matrix. To exclude cross-reactivity of antibodies as the source of unspecific IPs, one of the interaction partners was expressed as a FLAG-tagged protein, and precipitation was carried out with the highly specific and potent anti-FLAG M2 antibody. Transfection conditions were adjusted to give comparable expression levels of BARD1 and FLAG-EWS, as well as FLAG-BARD1 and EWS-FLI1

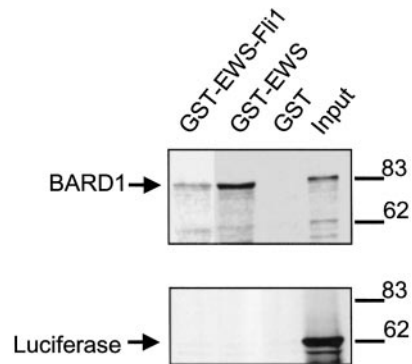


Fig. 1. GST pull-down of ³⁵S-labeled BARD1. GST, GST-EWS, and GST-EWS-FLI1 fusion proteins were incubated with *in vitro*-translated, ³⁵S-labeled BARD1 or firefly luciferase. BARD1 but not firefly luciferase was specifically retained by GST-EWS and GST-EWS-FLI1. Twenty times more ³⁵S-labeled BARD1 has been included in the GST pull-down reactions than loaded in the input lane.

proteins (Fig. 2, lysates). EWS-FLI1 precipitated with FLAG-tagged BARD1 (Fig. 2A), and BARD1 specifically coprecipitated with FLAG-tagged EWS (Fig. 2B). Only a weak signal was obtained for coprecipitation of endogenous BARD1 with FLAG-EWS due to the much lower abundance of the endogenous protein relative to the amount of ectopically expressed BARD1 in transfected cells. No association or precipitation was detectable with no antibody or irrelevant antibody. The reciprocal precipitation experiments did not give any conclusive results because precipitation of FLAG-tagged EWS-FLI1 was inefficient, and untagged EWS tended to stick to the precipitation matrix (data not shown).

Further proof of the interactions between EWS and EWS-FLI1 with BARD1 was obtained by coimmunoprecipitation of the endogenous complexes. As demonstrated in Fig. 3 BARD1 antibodies specifically coprecipitated EWS from HeLa cells (Fig. 3A) and EWS-FLI1 from EWS-negative STA-ET-7.2 cells. (Fig. 3B).

Association of BARD1 with EWS and EWS-FLI1 in the Living Cell. FRET microscopy was applied to confirm and localize the interaction of BARD1 with EWS and EWS-FLI1 in the living cell. The method is based on energy transfer between a donor fluorophore (CFP) and an acceptor fluorophore (YFP) with overlapping emission/excitation spectra that is restricted to close spatial proximity (distance not exceeding 10 nm). A close association of two proteins fused to the respective fluorophores results in an increase of acceptor fluorescence (measurable by ratio imaging) and quenching of the donor fluorescence (measurable by donor recovery after acceptor photo-bleaching; Ref. 10). To investigate the interaction of BARD1 with EWS and EWS-FLI1, we applied acceptor photo-bleaching FRET microscopy, which, although less sensitive than ratio imaging, does not require a complete colocalization or identical expression levels of the proteins and is not prone to false positive signals. In parallel, transfections were carried out with a CYFP tandem fusion, resulting in constitutive FRET as a positive control and uncoupled CFP and YFP proteins unable to interact with each other as a negative control. Because cotransfected cells frequently showed signs of apoptosis, presumably due to BARD1 overexpression, only living cells were evaluated for FRET. Results are presented in Fig. 4. The YFP and CFPpre (CFP image before acceptor photo-bleaching) images monitor the distribution of YFP- and CFP-coupled proteins in the cell. EWS- and EWS-FLI1-fluorophore fusion proteins were restricted to the nucleus, sparing the nucleoli, whereas BARD1 fusion proteins were observed in the nucleus as well as in the cytoplasm. In addition, BARD1 was occasionally observed in nuclear speckles (data not shown). The image CFPpost was taken after destruction of the YFP acceptor fluorophore

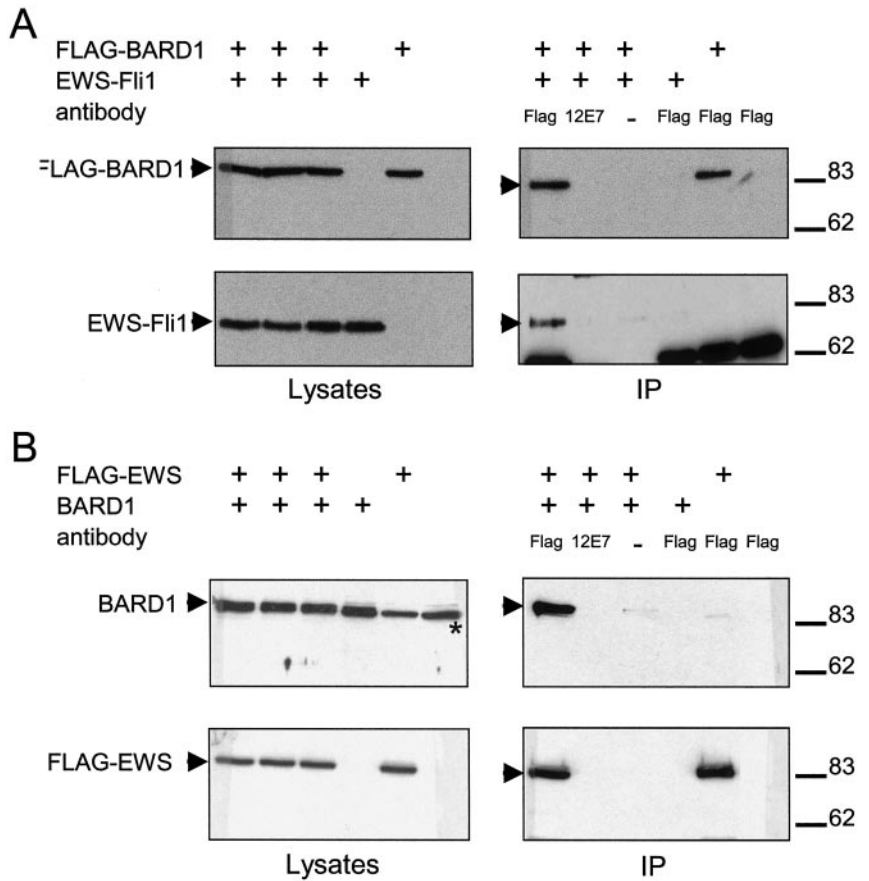


Fig. 2. IPs of ectopically expressed BARD1 with EWS and EWS-FLI1. *A*, coprecipitation of EWS-FLI1 with FLAG-BARD1. *B*, coprecipitation of BARD1 with FLAG-EWS. SJ-NB7 cells were transfected with expression plasmids for FLAG-EWS and BARD1, respectively, for FLAG-BARD1 and EWS-FLI1 as indicated on top of the figure, and relative expression levels of ectopically expressed proteins were monitored on Western blots of whole cell lysates (*left panels*). IPs were performed using Dynabeads coated with the indicated antibodies, and immunocomplexes were resolved on 8.5% polyacrylamide gels. *Left panels*, Western blots of cell lysates to control for protein expression. The asterisks indicates endogenous BARD1 protein, which was slightly smaller than ectopically expressed BARD1, presumably due to the use of an alternative start codon. *Right panels*, Western blot of precipitated immunocomplexes.

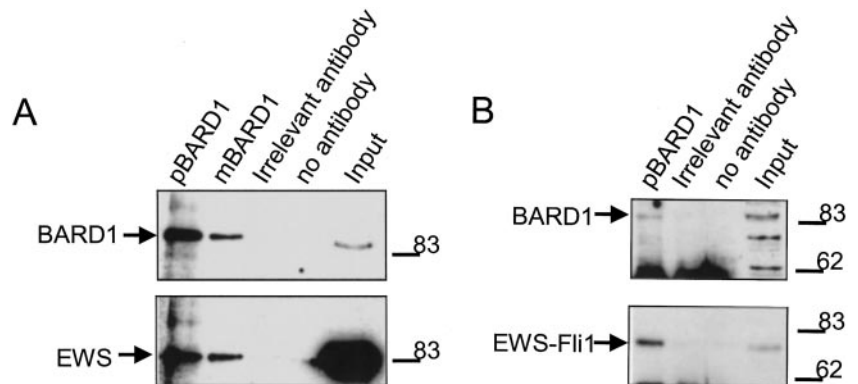
by constant illumination through the YFP filter set, with the same camera settings as the CFPre image before bleaching. The ratio of the CFPost and CFPre images was electronically calculated and represented by a ratio image. A clear FRET signal was obtained for the CYFP fusion protein but not for the negative control. For cotransfection of CFP-EWS-FLI1 with YFP-BARD1 and of CFP-BARD1 with YFP-EWS, a weak but reproducibly positive nuclear ratio image was obtained in a subset of transfected cells, confirming at least occasional association between BARD1 and EWS as well as EWS-FLI1 in the living cell.

Discussion

In this study we provide evidence for the interaction of the minimal EWS transforming domain with the putative tumor suppressor protein BARD1 in the context of germ-line EWS and EWS-FLI1, suggesting

a possible link between these proteins and the breast cancer susceptibility gene *BRCA1*. Whereas GST pull-down assays and FRET microscopy suggest a stronger interaction between BARD1 and EWS than between BARD1 and EWS-FLI1, IP experiments do not support this notion. However, the different experimental approaches provide complementary qualitative rather than quantitative information. BARD1 was identified by its interaction with the tumor suppressor protein BRCA1, which is mutated in about 80% of hereditary breast cancer cases and plays an important role in recombination repair and checkpoint control (for review, see Ref. 13). Both proteins interact via their NH₂-terminal RING domains, whereas communication with the EWS NH₂ terminus involves the COOH-terminal portion of BARD1 comprising two of the three ankyrin repeats and the BRCT domain. Within the EWS NH₂ terminus, deletion analysis indicated that the BARD1 interaction surface does not coincide with the epitope binding

Fig. 3. Precipitation of endogenous complexes containing BARD1 with EWS and with EWS-FLI1. *A*, the complex of EWS and BARD1 was precipitated from whole HeLa cell extract with anti-BARD1 669D polyclonal antiserum (*pBARD1*) and anti-BARD1 EE6 monoclonal antibody (*mBARD1*), and the proteins contained were detected on the Western blot with anti-EWS 677 and anti-BARD1 669D. *B*, the complex between BARD1 and EWS-FLI1 was precipitated from nuclear extracts of STA-ET-7.2 cells using anti-BARD1 669D (*pBARD1*), and proteins were detected on the Western blot by probing with anti-FLI1 C19 and anti-BARD1 669D. EWS-FLI1 coprecipitates specifically with BARD1, but not with no antibody or irrelevant (anti-KAI1) antibody. Fifteen times more protein was included in the IP reactions than applied to the gel in the input lane.



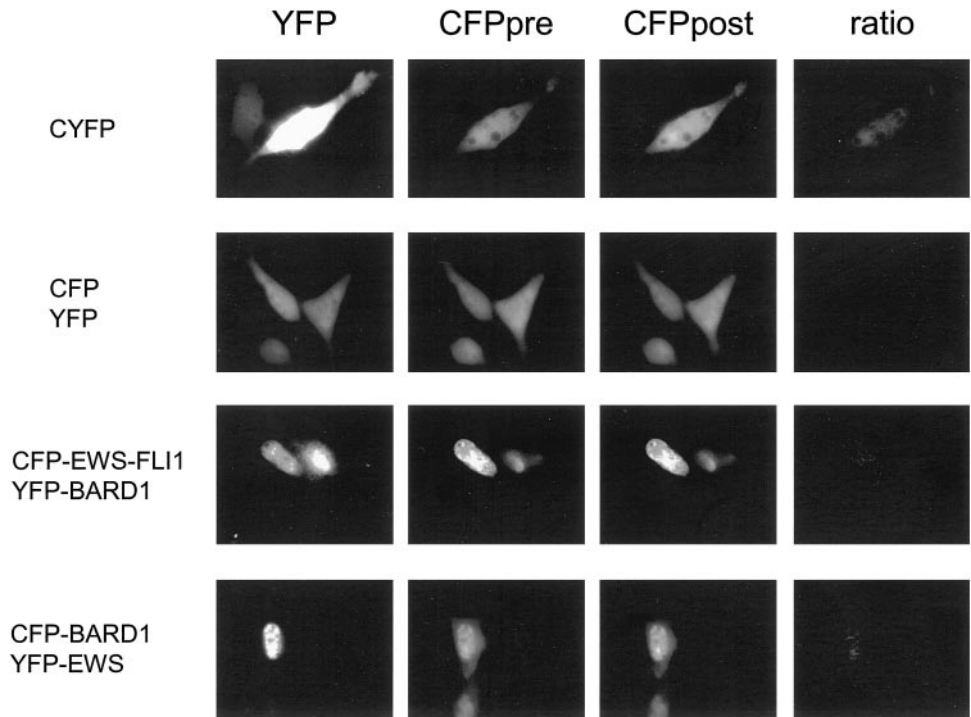


Fig. 4. Association of BARD1 with EWS or EWS-FLI1 in the living cell. Cells were transfected with indicated expression constructs. Fixed cells on coverslips were analyzed by acceptor photobleaching FRET microscopy. *YFP* and *CFPpre*, images taken with the respective filter sets before bleaching. *CFPost*, CFP image taken after photobleaching. *Ratio*, calculated ratio image of *CFPost*/*CFPpre*. The CYFP tandem fusion results in constitutive FRET, represented by a positive ratio image. CFP and YFP proteins are unable to interact and therefore show a blank ratio image. Coexpression of YFP-BARD1 with CFP-EWS-FLI1 and of YFP-EWS with CFP-BARD1 results in a weak but positive ratio image, indicating FRET and association of the two proteins in the living cell.

to hsRBP7 (Ref. 6; data not shown). Thus, it is possible that EWS and EWS-FLI1 are involved in higher order protein complexes linking transcriptional regulation to RNA processing and genome surveillance. The function of BRCA1 in DNA repair and maintenance of genome integrity is well established (13). BARD1 can be found together with BRCA1 and hsRad51 in nuclear foci during S phase of the cell cycle (14). These three proteins, together with proliferating cell nuclear antigen, also cluster in foci after DNA damage, compatible with a role in replication-associated repair of DNA damage (15). Interestingly, our FRET results indicate association of EWS and EWS-FLI1 with BARD1 in nuclear granular structures. The link of BARD1 to DNA repair may be provided by its interaction with CstF50, a subunit of the cleavage stimulation factor involved in polyadenylation of RNA. After DNA damage, polyadenylation of the nascent RNA is inhibited at the cleavage step upon interaction of CstF50 with BARD1 (11, 16). It has been speculated that this inhibitory mechanism prevents premature RNA maturation at cryptic polyadenylation sites, which may be caused by pausing of RNA polymerase II at sites of DNA damage. One may speculate that EWS-FLI1 targets BARD1 specifically to certain ets-responsive genes recruiting CstF50 and blocking proper RNA processing. As a consequence, EWS-FLI1 might negatively regulate gene expression posttranscriptionally on the level of RNA maturation.

A link between TET family proteins and double-strand DNA repair may be provided by TLS knockout mice, which suffer from pronounced genomic instability with frequent chromosomal breakage, centromeric fusions, and extrachromosomal elements (17). Because EWS-deficient mice have not been generated thus far, a possibly similar role of EWS in DNA repair remains to be demonstrated. Intriguingly, EFTs have long been known as particularly radiosensitive tumors, a characteristic that, in breast cancer patients, is associated with BRCA1 deficiency.

Apoptotic cell death has recently been demonstrated to be accompanied by an increase in BARD1 levels, and ectopic overexpression of BARD1 was found to result in apoptotic cell death (18). Conversely, BARD1-repressed cells show a growth reduction and are defective for

the apoptotic response to genotoxic stress. The apoptotic activity of BARD1 involves binding to and elevations of p53 independent of BRCA1, which was found to partially counteract BARD1-induced cell death. Similarly, repression of EWS-FLI1 expression in EFT cells results in growth reduction (for review, see Ref. 1), but ectopic expression of EWS-FLI1 in a non-EFT background is toxic to most cell types. However, loss of *p53* or *INK4A* gene function may rescue EWS-FLI1 transgenic cells from apoptosis, compatible with a role for an impaired p53/p14^{ARF} pathway in EWS-FLI1-mediated transformation (19). In contrast, p53 mutations are rare in primary EFT cells (20), and loss of *INK4A* gene activity is observed in only about 30% of cases (21). Thus, if tolerance to EWS-FLI1 expression generally requires a defect in the p53/p14^{ARF} pathway, it must occur at a different level in the majority of EFTs. Components of the BRCA1-associated genome surveillance complex (BASC; Ref. 22) may constitute interesting candidates for such a defect.

EWS-FLI1 has been demonstrated to repress a multitude of genes (2) including the *TGF β R2* gene (23) by an unknown mechanism. It is intriguing to speculate that BARD1 may play a role in this activity because its partner BRCA1 interacts with components of the histone deacetylase complex (24). In fact, in preliminary reporter gene studies using the *TGF β R2* promoter, BARD1 significantly supported EWS-FLI1-mediated repression. However, this effect could not be unequivocally linked to the presence of the EWS NH₂ terminus because BARD1 also repressed germ-line FLI1-mediated activation of this promoter, depending on the cell line used (data not shown). Similar inconsistent results were obtained using an EWS-FLI1-activated promoter (data not shown). These observations may be explained by induction of apoptosis as a consequence of ectopic BARD1 expression.

The BRCA1/BARD1 heterodimer constitutes an E3 ubiquitin ligase (25), which has auto-ubiquitination activity and mediates mono-ubiquitination of histone H2A and phosphorylated histone H2A(X) *in vitro* (26). It has been assumed that mono-ubiquitination serves a regulatory function other than signaling for proteasomal degradation. The modification of histones H2A and H2A(X) by BRCA1/BARD1 may be

linked to chromatin remodeling processes occurring during DNA repair (25). Because the interactions with BRCA1 and the EWS NH₂ terminus occur at different epitopes on BARD1, EWS and EWS-FLI1 probably do not interfere with this function. It remains to be demonstrated whether EWS or EWS-FLI1 is ubiquitinated by the BRCA1/BARD1 complex. However, no influence of BARD1 on EWS or EWS-FLI1 protein stability or *vice versa* was observed (data not shown), excluding an influence of the communication between these proteins on their mutual turnover via the proteasome pathway.

In summary, the interaction of EWS and EWS-FLI1 with BARD1 described here may identify an important role for the BRCA1 tumor suppressor pathway in EFT pathogenesis. However, the mechanism for its functional involvement remains to be elucidated.

Acknowledgments

We thank O. Delattre (Institut Curie, Paris, France), C. Denny (University of California Los Angeles, Los Angeles, CA), and R. Baer (Columbia University, New York, NY) for supplying antibodies to EWS and BARD1.

References

- Arvand, A., and Denny, C. T. Biology of EWS/ETS fusions in Ewing's family tumors. *Oncogene*, *20*: 5747–5754, 2001.
- Arvand, A., Welford, S. M., Teitell, M. A., and Denny, C. T. The COOH-terminal domain of FLI-1 is necessary for full tumorigenesis and transcriptional modulation of EWS-FLI-1. *Cancer Res.*, *61*: 5311–5317, 2001.
- Lessnick, S. L., Braun, B. S., Denny, C. T., and May, W. A. Multiple domains mediate transformation by the Ewing's sarcoma EWS/FLI-1 fusion gene. *Oncogene*, *10*: 423–431, 1995.
- Welford, S. M., Hebert, S. P., Deneen, B., Arvand, A., and Denny, C. T. DNA binding domain-independent pathways are involved in EWS/FLI1-mediated oncogenesis. *J. Biol. Chem.*, *276*: 41977–41984, 2001.
- Knoop, L. L., and Baker, S. J. EWS/FLI alters 5'-splice site selection. *J. Biol. Chem.*, *276*: 22317–22322, 2001.
- Petermann, R., Mossier, B. M., Aryee, D. N., Khazak, V., Golemis, E. A., and Kovar, H. Oncogenic EWS-FlI1 interacts with hSRPB7, a subunit of human RNA polymerase II. *Oncogene*, *17*: 603–610, 1998.
- Bertolotti, A., Melot, T., Acker, J., Vigneron, M., Delattre, O., and Tora, L. EWS, but not EWS-FLI-1, is associated with both TFIID and RNA polymerase II: interactions between two members of the TET family, EWS and hTAFII68, and subunits of TFIID and RNA polymerase II complexes. *Mol. Cell Biol.*, *18*: 1489–1497, 1998.
- Wu, L. C., Wang, Z. W., Tsan, J. T., Spillman, M. A., Phung, A., Xu, X. L., Yang, M. C., Hwang, L. Y., Bowcock, A. M., and Baer, R. Identification of a RING protein that can interact *in vivo* with the BRCA1 gene product. *Nat. Genet.*, *14*: 430–440, 1996.
- Kovar, H., Jug, G., Hattinger, C., Spahn, L., Aryee, D. N., Ambros, P. F., Zoubek, A., and Gardner, H. The EWS protein is dispensable for Ewing tumor growth. *Cancer Res.*, *61*: 5992–5997, 2001.
- Schmid, J. A., Scholze, P., Kudlacek, O., Freissmuth, M., Singer, E. A., and Sitte, H. H. Oligomerization of the human serotonin transporter and of the rat GABA transporter 1 visualized by fluorescence resonance energy transfer microscopy in living cells. *J. Biol. Chem.*, *276*: 3805–3810, 2001.
- Kleiman, F. E., and Manley, J. L. Functional interaction of BRCA1-associated BARD1 with polyadenylation factor CstF-50. *Science (Wash. DC)*, *285*: 1576–1579, 1999.
- Lassar, A. B., Davis, R. L., Wright, W. E., Kadesch, T., Murre, C., Voronova, A., Baltimore, D., and Weintraub, H. Functional activity of myogenic HLH proteins requires hetero-oligomerization with E12/E47-like proteins *in vivo*. *Cell*, *66*: 305–315, 1991.
- Venkataraman, A. R. Functions of BRCA1 and BRCA2 in the biological response to DNA damage. *J. Cell Sci.*, *114*: 3591–3598, 2001.
- Jin, Y., Xu, X. L., Yang, M. C., Wei, F., Ayi, T. C., Bowcock, A. M., and Baer, R. Cell cycle-dependent colocalization of BARD1 and BRCA1 proteins in discrete nuclear domains. *Proc. Natl. Acad. Sci. USA*, *94*: 12075–12080, 1997.
- Scully, R., Chen, J., Ochs, R. L., Keegan, K., Hoekstra, M., Feunteun, J., and Livingston, D. M. Dynamic changes of BRCA1 subnuclear location and phosphorylation state are initiated by DNA damage. *Cell*, *90*: 425–435, 1997.
- Kleiman, F. E., and Manley, J. L. The BARD1-CstF-50 interaction links mRNA 3' end formation to DNA damage and tumor suppression. *Cell*, *104*: 743–753, 2001.
- Hicks, G. G., Singh, N., Nashabi, A., Mai, S., Bozek, G., Klewes, L., Arapovic, D., White, E. K., Koury, M. J., Oltz, E. M., Van Kaer, L., and Ruley, H. E. Fus deficiency in mice results in defective B-lymphocyte development and activation, high levels of chromosomal instability and perinatal death. *Nat. Genet.*, *24*: 175–179, 2000.
- Irminger-Finger, I., Leung, W. C., Li, J., Dubois-Dauphin, M., Harb, J., Feki, A., Jefford, C. E., Soriano, J. V., Jaconi, M., Montesano, R., and Krause, K. H. Identification of BARD1 as mediator between proapoptotic stress and p53-dependent apoptosis. *Mol. Cell*, *8*: 1255–1266, 2001.
- Deneen, B., and Denny, C. T. Loss of p16 pathways stabilizes EWS/FLI1 expression and complements EWS/FLI1 mediated transformation. *Oncogene*, *20*: 6731–6741, 2001.
- Kovar, H., Auinger, A., Jug, G., Aryee, D., Zoubek, A., Salzer-Kuntschik, M., and Gardner, H. Narrow spectrum of infrequent p53 mutations and absence of MDM2 amplification in Ewing tumours. *Oncogene*, *8*: 2683–2690, 1993.
- Kovar, H., Jug, G., Aryee, D. N., Zoubek, A., Ambros, P., Gruber, B., Windhager, R., and Gardner, H. Among genes involved in the RB dependent cell cycle regulatory cascade, the *p16* tumor suppressor gene is frequently lost in the Ewing family of tumors. *Oncogene*, *15*: 2225–2232, 1997.
- Wang, Y., Cortez, D., Yazdi, P., Neff, N., Elledge, S. J., and Qin, J. BASC, a super complex of BRCA1-associated proteins involved in the recognition and repair of aberrant DNA structures. *Genes Dev.*, *14*: 927–939, 2000.
- Hahm, K. B., Cho, K., Lee, C., Im, Y. H., Chang, J., Choi, S. G., Sorensen, P. H., Thiele, C. J., and Kim, S. J. Repression of the gene encoding the TGF- β type II receptor is a major target of the EWS-FLI1 oncoprotein. *Nat. Genet.*, *23*: 222–227, 1999.
- Yarden, R. I., and Brody, L. C. BRCA1 interacts with components of the histone deacetylase complex. *Proc. Natl. Acad. Sci. USA*, *96*: 4983–4988, 1999.
- Hashizume, R., Fukuda, M., Maeda, I., Nishikawa, H., Oyake, D., Yabuki, Y., Ogata, H., and Ohta, T. The RING heterodimer BRCA1-BARD1 is a ubiquitin ligase inactivated by a breast cancer-derived mutation. *J. Biol. Chem.*, *276*: 14537–14540, 2001.
- Chen, A., Kleiman, F. E., Manley, J. L., Ouchi, T., and Pan, Z. Q. Auto-ubiquitination of the BRCA1/BARD1 RING ubiquitin ligase. *J. Biol. Chem.*, *277*: 22085–22092, 2002.